XVIII[èmes] Journées Nationales Génie Côtier – Génie Civil
Anglet, 2024
DOI:10.5150/jngcgc.2024.003 *© Editions Paralia CFL*
disponible en ligne – http://www.paralia.fr – available online

Dynamics of infragravity waves at a dissipative beach under paroxysmal conditions

Xavier BERTIN [1], Nushrat YEASMIN [1]

1. UMR 7666 LIENSs, CNRS-La Rochelle Université, 2 rue Olympe de gouges, 17000, La Rochelle, France.
xbertin@univ-lr.fr

Abstract:
Infragravity (hereafter IG) waves are long waves with periods of the order of the minute and related to the presence of groups in the incident short waves. IG waves were the subject of numerous studies at sandy beaches and it is now well acknowledged that they have a key contribution to the hydro-sedimentary dynamics of coastal zones during storms. Yet, while the existing literature suggests that for a given incident sea state, IG waves should be larger at gently sloping beaches, the largest IG waves were rather observed under storm waves over steep bottoms. This apparent inconsistency suggests that additional processes controlling IG waves could be relevant under paroxysmal conditions. In order to explore such processes, we present the analysis of bottom pressure collocated with current velocity data collected along a cross-shore transect located to the Southwest of Oléron Island. The analysis of this data revealed a contrasting behaviour between moderate-energy wave conditions, where IG waves continuously grow towards the shore and storm wave conditions, where they decay across the surfzone. The second behaviour is explained by the modulation of short-wave heights by IG waves in the surfzone, which creates a positive correlation between IG waves and the energy envelope of short waves. This pattern causes the work done radiation stress of the short waves to contribute negatively to IG waves. This new physical process has important implications and is being further quantified by means of wave phase-resolving modelling.

Keywords:
Hydrodynamics under storm, Infragravity waves, Dissipative beach, Oléron Island.

1. Introduction

Infragravity (hereafter IG) waves correspond to long surface waves with periods of the order of one minute and related to the presence of groups in the incident short waves (see BERTIN *et al*., 2018 for a review). IG waves were described for the first time in the middle of the 20th century (MUNK, 1949) and were the subject of numerous studies, particularly at sandy beaches. It is nowadays well acknowledged that IG waves have a key contribution to the hydro-sedimentary dynamics of coastal zones during storms,

namely at dissipative beaches, where they dominate the variance of the free surface elevation along the shoreline (BERTIN *et al*., 2018). Yet, while the existing literature suggests that, for a given incident sea state, IG waves should be larger at gently sloping beaches (e.g. DE BAKKER *et al*., 2016; LI *et al*., 2020), the largest IG waves were rather reported under storm waves over steep bottoms (e.g. SHEREMET *et al*., 2014; MATSUBA *et al*., 2021). This apparent inconsistency suggests that additional processes could be at play during storms and paroxysmal conditions.

In order to better understand the dynamics of IG waves under storm waves, this study takes advantage of bottom pressure and current velocity data collected since 2021 in the shoreface of a dissipative beach located to the southwest of Oléron Island, in the scope of the national observation service DYNALIT (https://www.dynalit.fr/). These permanent deployments allow to monitor the sea-state under paroxysmal conditions, where field data are very scarce in the international literature. The next section presents the study area, followed by a section describing data collection and processing. Section 4 presents the results of data analysis and the last section concludes on the implications and perspectives of this study.

2. Study area

The study area is located to the Southwest of Oléron Island, in the middle of the Bay of Biscay, and corresponds to a dissipative beach (mean slope of O(1:100)). Its shoreface is characterised by a very mild slope of O(1:1000), the 20 m isobath line being found about 10 km from the shoreline (PEZERAT *et al*., 2022). This beach is made of fine sands (d_{50}~0.2 mm) and is usually longshore-uniform, with poorly developed three-dimensional features (BERTIN *et al*., 2020). The local tidal regime is semi-diurnal and ranges from 1.5 m to 5.5 m (DODET *et al*., 2019). The wave regime is energetic, with yearly-mean wave conditions by 30 m water depth characterized by a spectral significant height (hereafter H_{m0}) of 1.6 m, a mean wave period (hereafter T_{m02}) of 7.2 s and a mean direction of 285◦ (DODET *et al*., 2019). However, measurements carried out in the shoreface 3 km from shore revealed that H_{m0} can exceed 6 m with peak period (hereafter T_p) over 20 s during storms (GUERIN *et al*., 2018; PEZERAT *et al*., 2022). Under such conditions, very large IG waves develop, with $H_{m0,IG}$ over 1.5 m observed along the beach (BERTIN *et al*., 2020).

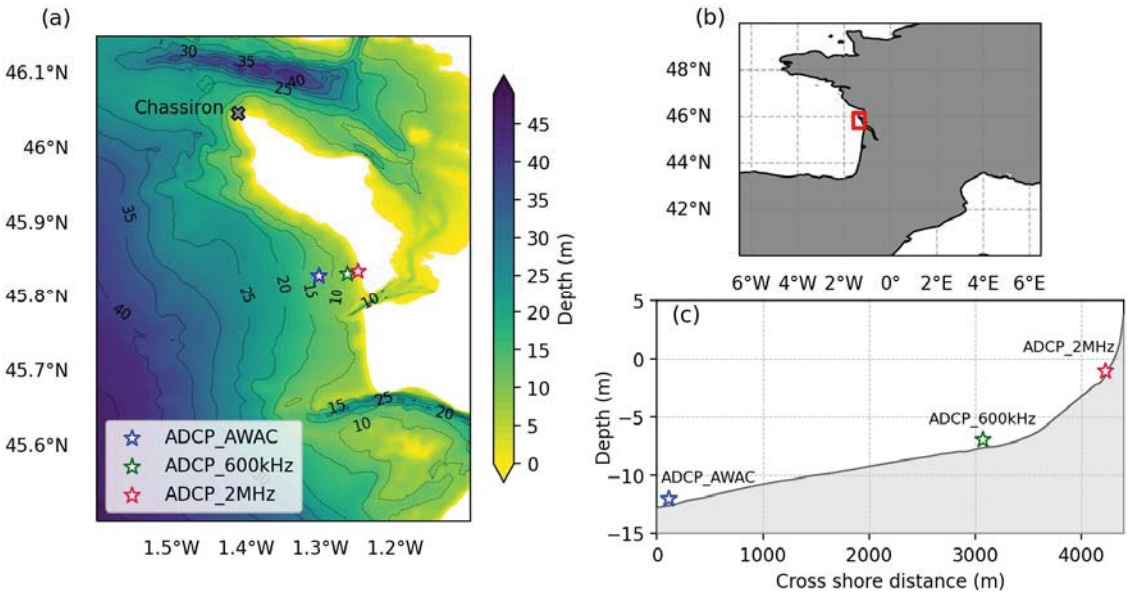

Figure 1. (a) Bathymetric map of the study area, (b) location of the study area in the Bay of Biscay and (c) cross-shore bathymetric profile showing the location of the three sensors used in this study.

3. Data collection and processing

In order to evaluate the feasibility of permanent deployment of bottom pressure sensors in the scope of the national observation service DYNALIT, a field campaign was carried out between January and February 2021. This period allowed recording very energetic hydrodynamic conditions, namely during storm Justine, which produced waves of H_{m0} of the order of 10 m in the Bay of Biscay (PEZERAT *et al*., 2022). A high resolution (1MHz) Acoustic Wave and Current profiler (AWAC) was deployed by 12.8 m below mean sea-level (hereafter MSL), a 600 kHz Acoustic Doppler Current Profiler (hereafter ADCP) was deployed by 8 m below MSL and a high resolution (2 MHz) ADCP was deployed in the intertidal zone, 1.5 m below MSL (see Figure 1 and PEZERAT et al., 2022 for more details). A hydrostatic reconstruction of the free surface elevation was first performed based on bottom pressure data corrected from atmospheric pressure. A transfer function method based on linear theory (BISHOP & DONELAN, 1987) was applied to reconstruct the free surface elevation signal. A high frequency cutoff of 0.25 Hz was used for the whole dataset to prevent the over-amplification of the high-frequency noise. Finally, power spectral densities were computed using 9 Hanning-windowed, 50% overlapping segments. Standard wave bulk parameters such as H_{m0}, T_{m02} and the continuous peak period T_{pc}, were computed using spectral moments, defined as:

$$m_n = \int_{f_{min}}^{f_{max}} f^n E(f) df \qquad (1)$$

For the gravity band, f_{max} was set to 0.25 Hz as explained above and f_{min} is adaptive and defined as half the continuous peak frequency following BERTIN *et al.*, (2020). For the IG band, spectral moments where integrated between 0.0078 Hz, the first resolved frequency and f_{min} as defined above. For the analysis of IG waves, the incoming and the outgoing elevation signals were separated using current velocities following the approach of VAN DONGEREN and SVENDSEN (1997), which corresponds to an extension of the approach of GUZA *et al.*, (1984) and is valid when dispersion is not negligible. This procedure allowed computing the incoming significant IG wave height, $H_{m0,IG+}$.

4. Results and discussion

4.1 Incident conditions

The studied period spans from the 29/01/2021 and the 31/01/2021 and encompasses the storm Justine, which generated waves of H_{m0} reaching about 10 m in the Bay of Biscay. At the location of the AWAC, H_{m0} rapidly increased from 2 m to 6 m while T_{pc} doubled from 11 to 22 s (Figure 2). In more details, H_{m0} was tidally modulated at the storm peak (Figure 2-b), revealing that the surfzone extended at least over 4 km at low tide (PEZERAT *et al.*, 2022). In terms of IG waves, $H_{m0,IG}$ increased from about 0.2 m to over 1.0 m.

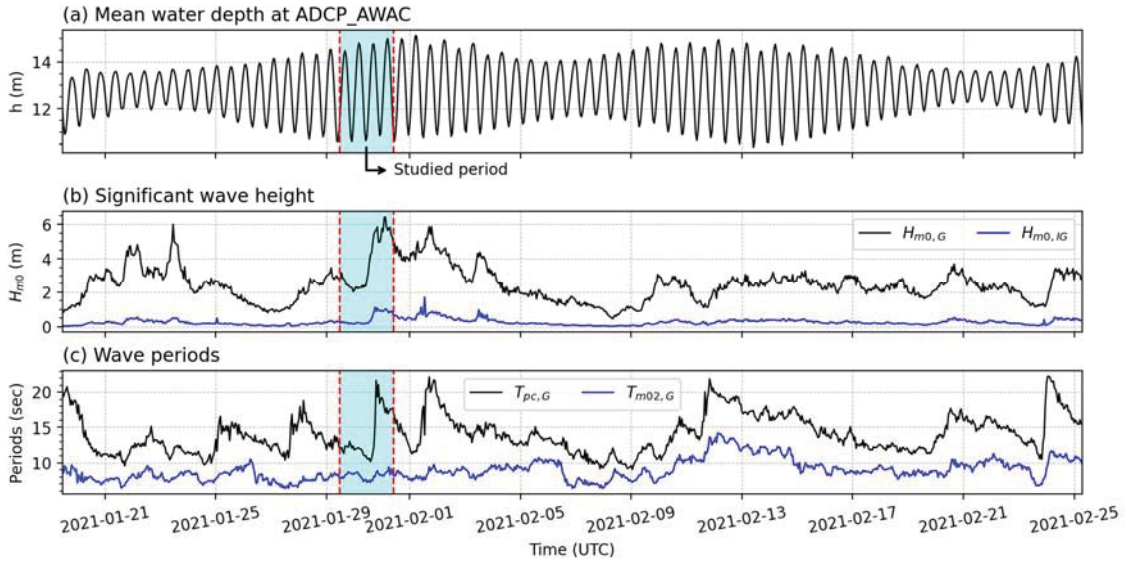

Figure 2. (a) Mean water depth, (b) H_{m0} in the gravity and IG ($H_{m0,IG}$) bands and T_{pc} and T_{m02} in the gravity band at the offshore-most sensor AWAC (see Figure 1).

4.2 Cross-shore evolution of IG waves:

Previous studies conducted at this beach (BERTIN *et al.*, 2020; PEZERAT *et al.*, 2023) reported that IG waves can be partly reflected along the shoreline, with a strong tidal

modulation, where reflection is very weak at low tide and almost full at high tide due to the presence of a steep berm in the beach upper part. As dealing with total signals that include incoming and outgoing IG waves considerably complicates the analysis, we only analysed the incoming signal in the following.

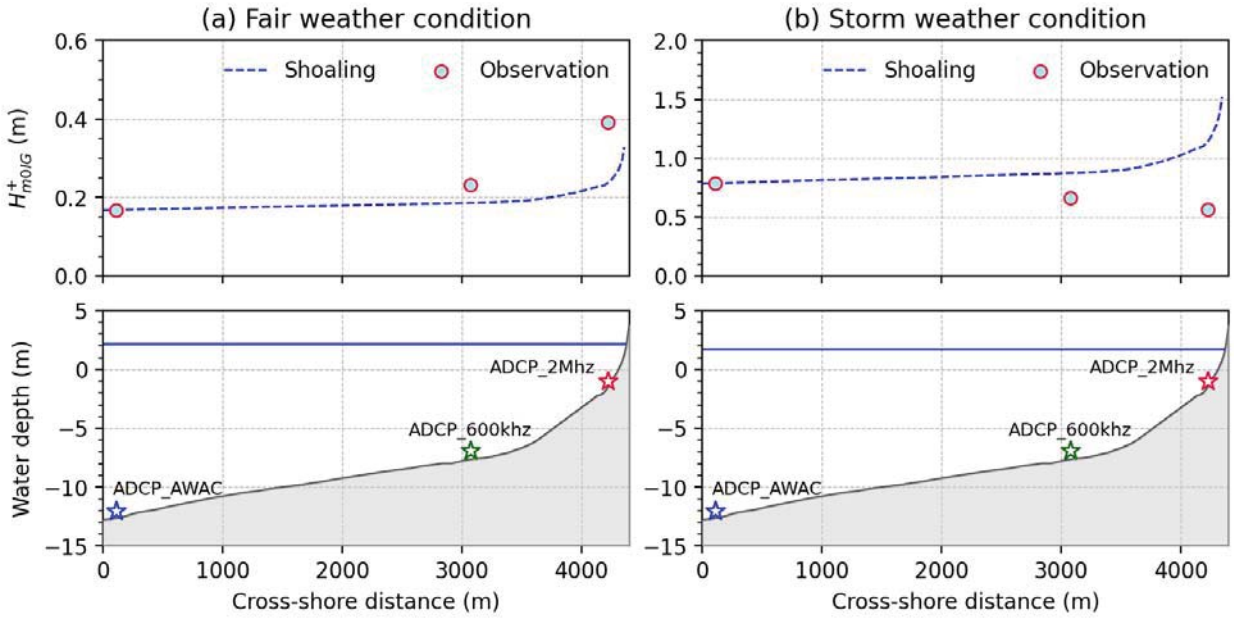

Figure 3. Observed cross-shore evolution of $H_{m0,IG+}$ against modeled assuming energy flux conservation (a) under fair-weather conditions (30/01/2021 at 4h00) and (b) under storm weather conditions (31/01/2021 at 3h00).

Under fair weather conditions (Figure 3a), $H_{m0,IG+}$ continuously increases towards the coast, at a rate larger than what would imply energy flux conservation (i.e. linear shoaling). This behaviour is classical for dissipative beaches, where IG waves are generated mostly through the bound wave mechanism and the mild slope implies that non-linear energy transfers from the short waves to the IG waves accumulate over long distance (DE BAKKER *et al.*, 2016; LIAO *et al.*, 2019). Surprisingly, a totally different pattern is observed under storm waves, where $H_{m0,IG+}$ continuously decreases towards the shoreline, and is almost halved along the coast compared to the shoreface (Figure 3b).

4.3 The cause for IG wave decay across wide surfzones

The decay of IG waves across the surfzone described in the previous section was already reported in several studies, either based on field experiments (DE BAKKER *et al.*, 2014) or phase-resolving wave modelling (RUJU *et al.*, 2018; RIJNSDORP *et al.*, 2022). These authors attributed IG wave decay towards the shore to dissipation by

breaking in very shallow depth (i.e. less than 1 m) and to a lesser extent, by bottom friction. In the present study, IG wave decay already occurs in the outer surfzone, by water depths of about 10 m (Figure 3-b). By such water depth, the observed IG wave decay cannot be attributed to dissipation by breaking while dissipation by bottom friction could only have a minor contribution.

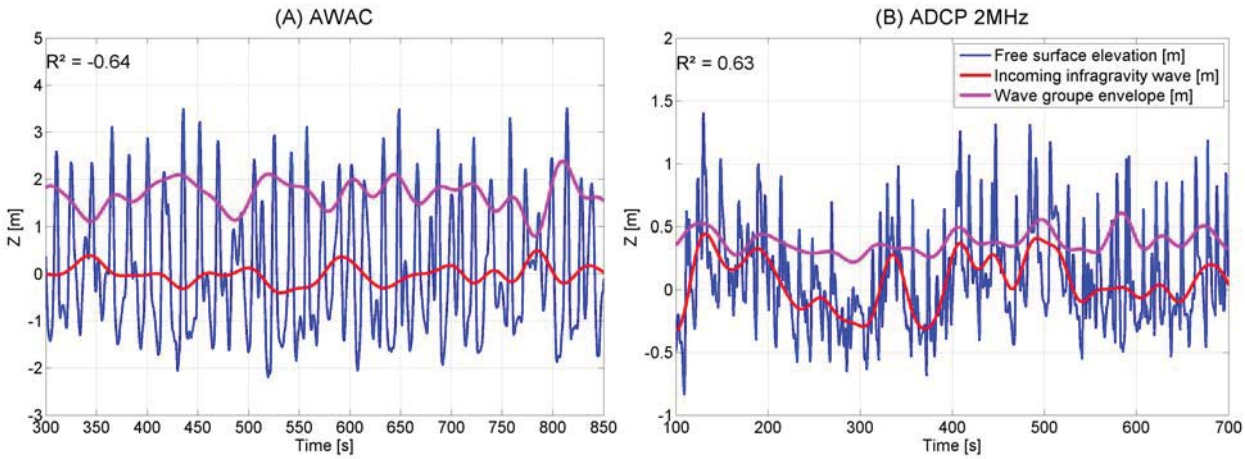

Figure 4. Sample of free surface elevation linearly reconstructed (blue), IG wave (red) and wave group envelope (magenta) at the AWAC (A) and the 2MHz ADCP on the 31/01/2021 at 7h49,

In order to explain this intriguing behaviour, we compared the IG wave and the wave group envelope (hereafter WGE) signals around the peak of the storm at the AWAC, located in the shoaling zone, and at the ADCP 2MHz, located in the surfzone (Figure 4). In the shoaling zone, a negative correlation can be observed between both signals (Figure 4a), which corresponds to the bound wave pattern, first described by LONGUET-HIGGINS and STEWART (1962), where the work done by the radiation stress of the short waves results in energy transfers from the short waves to the IG waves. In the surfzone, an opposite behaviour is observed, where the IG waves and the WGE are in phase (Figure 4a). This pattern is explained by the depth-limitation breaking of the short waves, which is modulated by IG waves: short waves break less on the crest of IG waves than on the through of IG waves (TISSIER *et al.*, 2015; BERTIN *et al.*, 2020). In this pattern, the work done by radiation stress of the short waves has a negative contribution to the IG waves and we propose that it explains the observed decay of IG waves across the surfzone.

5. Conclusions and perspectives

This study presented field observation of bottom pressure and current velocities collected along the cross-shore profile of a dissipative beach under very energetic wave conditions. The analysis of the incoming IG wave signal revealed a contrasting

behaviour between fair weather conditions where the IG wave energy flux continuously increases towards the shore and storm conditions where the IG wave energy flux continuously decreases shoreward. Considering the water depth where this process takes place, it cannot correspond to IG wave dissipation. Alternatively, the comparison of the IG wave and the WEE signals revealed a positive correlation pattern in the surfzone, which causes the work done by radiation stresses of the short waves to contribute negatively to the IG waves. While this process should be active in any surfzone, we propose that it strongly impacts IG waves in the present case due to the very mild slope, which causes to negative contribution of the work done by the short-wave radiation stress to accumulate over long distance. The importance of this new process is being quantified using phase-resolving wave modelling, where model outputs are used to compute an energy flux conservation equation (e.g. RUJU *et al*., 2012).
Finally, it is nowadays well admitted that IG waves have a key contribution to coastal hazards during storms. This study suggests that, for a given sea state, IG waves would have a larger impact under paroxysmal conditions at coastal zones characterized by steep bottoms, such as volcanic islands.

Acknowledgements
The data used in this study were collected to the Southwest of Oléron Island in the scope of the national observation service DYNALIT. Nushrat Yeasmin was funded by the Research Infrastructure ILICO.

6. References

BERTIN X., DE BAKKER A., VAN DONGEREN A., *et al*., (2018). *Infragravity waves: From driving mechanisms to impacts*. Earth-Science Reviews, 177, 774–799. https://doi.org/10.1016/j.earscirev.2018.01.002

BERTIN X., MARTINS K., DE BAKKER A., CHATAIGNER T., GUERIN T., COULOMBIER T., DE VIRON O. (2020). *Energy transfers and reflection of infragravity waves at a dissipative beach under storm waves.* Journal of Geophysical Research: Oceans, 125(5), e2019JC015714. https://doi.org/10.1029/2019JC015714

BISHOP C. T., DONELAN M. A. (1987). *Measuring waves with pressure transducers.* Coastal Engineering, 11(4), 309–328. https://doi.org/10.1016/0378-3839(87)90031-7

DE BAKKER A.T.., TISSIER, M.F.S., RUESSINK B.G. (2014). *Shoreline dissipation of infragravity waves*. Continental Shelf Research, 72, 73–82. https://doi.org/10.1016/j.csr.2013.11.013

DE BAKKER A.T.M., TISSIER M.F.S., RUESSINK B.G. (2016). *Beach steepness effects on nonlinear infragravity-wave interactions: A numerical study*. Journal of Geophysical Research: Oceans, 121(1), 554–570. https://doi.org/10.1002/2015JC011268

DODET G., BERTIN X., BOUCHETTE F., GRAVELLE M., TESTUT L., WÖPPELMANN G. (2019). Characterization of Sea-level Variations Along the

Metropolitan Coasts of France: Waves, Tides, Storm Surges and Long-term Changes. Journal of Coastal Research; 88 (SI): 10–24. https://doi.org/10.2112/SI88-003.1

GUERIN T., BERTIN X., COULOMBIER, T., DE BAKKER A. (2018). *Impacts of wave-induced circulation in the surf zone on wave setup*. Ocean Modelling, 123, 86–97. https://doi.org/10.1016/j.ocemod.2018.01.006

GUZA R.T., THORNTON E.B., HOLMAN R.A. (1985). *Swash on steep and shallow beaches.* In Coastal Engineering 1984 (pp. 708-723). https://doi.org/10.1061/9780872624382.049

LI S., LIAO Z., LIU Y., OU Q. (2020). *Evolution of infragravity waves over a shoal under nonbreaking conditions*. Journal of Geophysical Research: Oceans, 125, e2019JC015864. https://doi.org/10.1029/2019JC015864

LONGUET-HIGGINSM.S., STEWART, R.W. (1962). *Radiation stress and mass transport in gravity waves, with application to "surf beats,"*. Journal of Fluid Mechanics 13, 481–504. https://doi.org/10.1017/S002211206

MATSUBA Y., SHIMOZONO T., TAJIMA Y. (2021). *Extreme wave runup at the Seisho Coast during Typhoons Faxai and Hagibis in 2019.* Coastal Engineering, 168, 103899. https://doi.org/10.1016/j.coastaleng.2021.103899

MUNK W. H. (1949). *Surf beat*. Eos Transactions, AGU, 30, 849–854. https://doi.org/10.1029/TR030i006p00849

PEZERAT M., BERTIN X., MARTINS K., LAVAUD L. (2022). *Cross-shore distribution of the wave-induced circulation over a dissipative beach under storm wave conditions.* Journal of Geophysical Research: Oceans, 127(3), e2021JC018108. https://doi.org/10.1029/2021JC018108

PEZERAT M., BERTIN X., COULOMBIER T. (2023). *Cross-shore suspended sediment transport in a macro-tidal and low-sloping upper shoreface.* Earth Surface Processes and Landforms, 48(5), 853-862. https://doi.org/10.1002/esp.5566

RIJNSDORP D.P., SMIT P.B., GUZA R.T. (2022). *A nonlinear, non-dispersive energy balance for surfzone waves: infragravity wave dynamics on a sloping beach.* Journal of Fluid Mechanics, 944, A45. https://doi.org/10.1017/jfm.2022.512

RUJU A., LARA J.L., LOSADA I.J. (2012). *Radiation stress and low-frequency energy balance within the surf zone: a numerical approach*. Coastal Engineering 68, 44–55. https://doi.org/10.1016/j.coastaleng.2012.05.003

SHEREMET A., STAPLES T., ARDHUIN F., SUANEZ S., ICHAUT, B. (2014). *Observations of large infragravity wave runup at Banneg Island, France.* Geophysical Research Letters, 41(3), 976–982. https://doi.org/10.1002/2013GL058880

TISSIER M., BONNETON, P., MICHALLET H., RUESSINK B.G. (2015). *Infragravity-wave modulation of short-wave celerity in the surf zone.* Journal of Geophysical Research: Oceans, 120(10), 6799–6814. https://doi.org/10.1002/2015JC010708

VAN DONGEREN A., SVENDSEN, I.A. (1997). *Absorbing-generating boundary condition for shallow water models.* Journal of Waterway, Port, Coastal, and Ocean Engineering, 123(6), 303–313. https://doi.org/10.1061/(ASCE)0733-950X(1997)123:6(303)